

Research Paper

PET of HER2 Expression with a Novel ^{18}F AI Labeled Affibody

Yuping Xu^{1,2}, Zhicheng Bai¹, Qianhuan Huang¹, Yunyun Pan¹, Donghui Pan², Lizhen Wang², Junjie Yan², Xinyu Wang¹, Runlin Yang², Min Yang^{1,2}✉

1. The First School of Clinical Medicine, Nanjing Medical University, Nanjing, Jiangsu, 210029, China;

2. Key Laboratory of Nuclear Medicine, Ministry of Health, Jiangsu Key Laboratory of Molecular Nuclear Medicine, Jiangsu Institute of Nuclear Medicine, Wuxi, Jiangsu, 214063, China.

✉ Corresponding author: yangmin@jsinm.org

© Ivyspring International Publisher. This is an open access article distributed under the terms of the Creative Commons Attribution (CC BY-NC) license (<https://creativecommons.org/licenses/by-nc/4.0/>). See <http://ivyspring.com/terms> for full terms and conditions.

Received: 2016.10.25; Accepted: 2017.02.24; Published: 2017.04.09

Abstract

Background: Human epidermal growth factor receptor type 2 (HER2) is abundant in a wide variety of tumors and associated with the poor prognosis. Radiolabeled affibodies are potential candidates for detecting HER2-positive lesions. However, laborious multiple-step synthetic procedure and high abdomen background may hinder the widespread use. Herein, cysteinylated ZHER_{2:342} modified with a new hydrophilic linker (denoted as MZHER_{2:342}) was designed and labeled using ^{18}F AI-NOTA strategies. The biologic efficacy of the novel tracer and its feasibilities for in vivo monitoring HER2 levels were also investigated in xenograft models with different HER2 expressions.

Method: MZHER_{2:342} was conjugated with MAL-NOTA under standard reaction conditions. The affibody molecule was then radiolabeled with ^{18}F AI complex. The binding specificity of the tracer, ^{18}F AI-NOTA-MAL-MZHER_{2:342}, with HER2 was primarily characterized via in vitro studies. MicroPET imaging were performed in nude mice bearing tumors (SKOV-3, JIMT-1 and MCF-7) after injection. The HER2 levels of xenografts were determined using Western blotting analysis.

Results: ^{18}F AI-NOTA-MAL-MZHER_{2:342} can be efficiently produced within 30 min with a non-decaycorrected yield of about 10% and a radiochemical purity of more than 95%. In vitro experiments revealed that the modified affibody retained the specific affinity to HER2. PET imaging showed that SKOV-3 and JIMT-1 xenografts were clearly visualized with excellent contrast and low abdomen backgrounds. On the contrary, the signals of MCF-7 tumor were difficult to visualize. The ROI values ranged from $16.54 \pm 2.69\%$ ID/g for SKOV-3 to $8.42 \pm 1.20\%$ ID/g for JIMT-1 tumors at 1h postinjection respectively. Poor uptake was observed from MCF-7 tumors with $1.71 \pm 0.34\%$ ID/g at the same time point. Besides, a significant linear correlation between % ID/g values and relative HER2 expression levels was also found.

Conclusions: ^{18}F AI-NOTA-MAL-MZHER_{2:342} is a promising tracer for in vivo detecting HER2 status with the advantages of facile synthesis and favorable pharmacokinetics. It may be useful in differential diagnosis, molecularly targeted therapy and prognosis of the cancers.

Key words: PET, HER2

Introduction

Human epidermal growth factor receptor-2 (HER2) is a 185-kDa transmembrane phosphoglycoprotein belonging to the EGFR family of tyrosine kinases. [1] It plays a key role in the proliferation, differentiation, and migration of cancer via two main signaling pathways (Ras/MAPK and PI3K). HER2 overexpression in cancers is correlated

with tumor aggressiveness and worse survival. Assessment of the receptor status is benefited for early detection of tumor recurrence, patient selection for molecularly targeted therapy and prognosis of the disease. [2, 3, 4]

Biopsy is the commonly used procedure to determine HER2 expression pattern by ex vivo,

however the sampled parts removal from the body may not properly represent the overall tumor characteristics due to heterogeneity of HER2 expression. [5] Non-invasive molecular imaging technology (e.g. SPECT, PET) provides a reliable strategy for in vivo determining HER2 expression via whole-body detection of abnormalities. Conventional ^{18}F -FDG PET has been widely employed for visualizing the cancer tissues according to increased glucose metabolism, while its ability to distinguish tumors with HER2 positive expression was disputed. [6,7]

^{89}Zr labeled anti-HER2 monoclonal antibodies such as ^{89}Zr -trastuzumab and ^{89}Zr -pertuzumab etc have been investigated to monitor HER2 levels in malignant tumors. [8,9] Although it showed good imaging properties, low tumor penetration, slow clearance and high radiation exposure preclude the clinical applications. [10,11] A small size targeting proteins, affibody molecules (~6.5 KDa), are alternative candidates for HER2 imaging with high specificity and rapid elimination. The high-contrast images could be obtained within several hours after injection of the radiolabeled affibodies, whereas it may take few days to clear backgrounds with antibodies. [12]

Several derives of a HER2-binding affibody, ZHER_{2:342}, have been developed and evaluated in preclinical and clinical SPECT and PET studies. [13, 14, 15-20] For example, ^{111}In -ABY-025 demonstrated noninvasive localization of metastases in patients with breast cancer. [17] Compared with SPECT, PET offers improved sensitivity, resolution and quantification. Various PET radioisotopes (^{68}Ga , ^{18}F) labeled affibody molecules have shown favorable performances. [19, 20, 21] Among these probes, the ^{18}F -labeled counterparts would be preferred for clinical use due to commercial availability and good imaging properties. Preclinical studies have shown that N-2-(4- ^{18}F fluorobenzamido) ethyl]maleimide labeled Cys-ZHER_{2:342} (^{18}F -FBEM-ZHER_{2:342}) is specific for detecting HER2-positive lesions and might be useful for monitoring changes of receptor expression to evaluate the response during therapy. [21, 22, 23]

However, high unspecific radioactivity accumulation was found to be kept for at least 1 hour in the liver after administration. [21] It may limit the potential for clinical application since the liver is a common metastatic site of cancer. A novel hydrophilic linker, Gly-Gly-Gly-Arg-Asp-Asn, significantly decreased the abdominal background at early time (nearly 30min) postinjection and efficiently improved the imaging qualities [24,25,26]. Thus, we hypothesized that a modified cysteinylated ZHER_{2:342}

affibody with the linker, denoted as MZHER_{2:342}, might possess more favorable in vivo pharmacokinetic performances.

Moreover, the synthesis of ^{18}F -FBEM-ZHER_{2:342} affibody is tedious for practical use. It requires multiple procedures to achieve the product including HPLC purification for two times. Recently, a simple strategy for preparing ^{18}F -labeled peptides developed by McBride et al via complexation of [^{18}F]aluminum fluoride with 1,4,7-triazacyclononanetricetic acid (NOTA) -derived peptide has been introduced for tumor imaging. [27, 28, 29] To facilitate the clinical translation, maleimide-NOTA (MAL-NOTA) conjugates of MZHER_{2:342} was designed and labeled with ^{18}F using the new one-step labeling method (Fig 1). The in vivo biological properties of the ^{18}F AI-labeled MZHER_{2:342} were investigated in a variety of tumor models and the correlations between quantitative PET data and HER2 status were also preliminarily evaluated.

Materials and Methods

General

All reagents were analytical grade and were obtained from commercial sources. Cys-ZHER_{2:342} and Cys-MZHER_{2:342} were custom made by Apeptide Co., Ltd. (Shanghai, China). MAL-NOTA was purchased from CheMatech (Dijon, France). No-carrier-added [^{18}F]fluoride was obtained from an in-house cyclotron (HM67, Sumitomo Heavy Industries, Ltd.) Analytic and preparative high-performance liquid chromatography (HPLC) were performed according to the previous literatures. [30,31]

The peptides was purified on a Waters high-performance liquid chromatography (HPLC) system with a Waters 2998 photodiode array detector (PDA) and a preparative C18 HPLC column (5 μm , 250 \times 19 mm, Waters Xbridge). The flow rate is 20ml/min, and the mobile phase changed from 95% solvent A (0.1% trifluoroacetic acid in water) and 5% solvent B (0.1% trifluoroacetic acid in acetonitrile) at 2min to 35% solvent A and 65% solvent B at 21min. The UV absorbance was monitored with the PDA detector at 218 nm.

A Waters Breeze system equipped with a Radiomatic 610TR flow scintillation analyzer (PerkinElmer), a Luna C18 column (5 μm , 250 \times 4.6 mm, Phenomenex) and a Waters 2487 dual λ absorbance detector was used for analyze the purities of the compounds. The buffer system were followed: buffer A, 0.1% v/v trifluoroacetic acid in water; buffer B, 0.1% v/v trifluoroacetic acid (TFA) in acetonitrile (ACN); and a gradient of 95% buffer A at 0-2 min to 35% buffer A at 35 min.

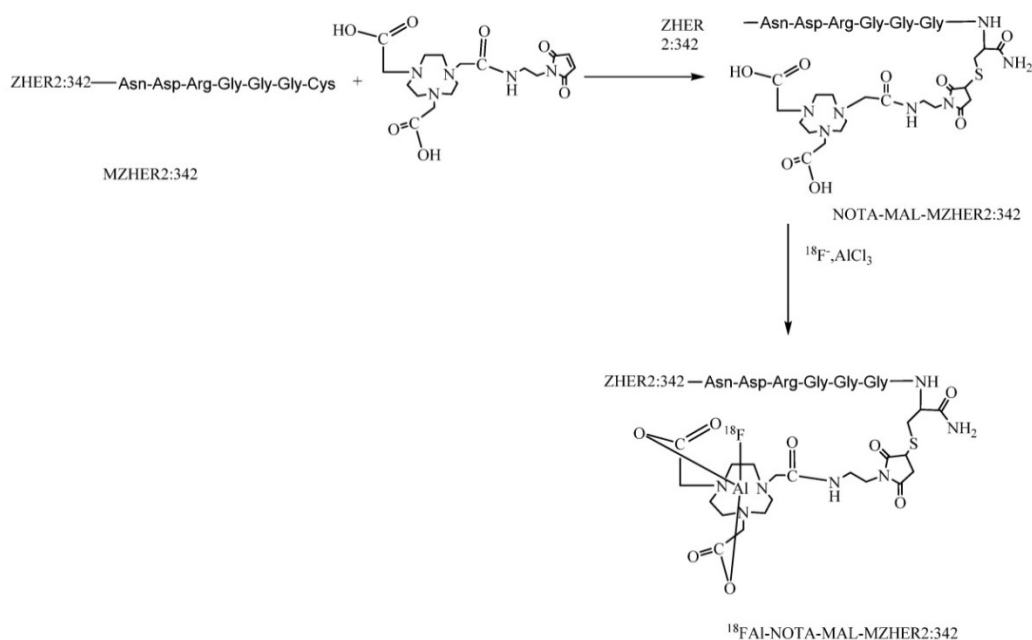


Figure 1. Schemes for radiosynthesis of ^{18}F -Al-NOTA-MAL-MZHER_{2:342}

Synthesis of NOTA-MAL-MZHER_{2:342}

Cys-MZHER_{2:342} were conjugated with MAL-NOTA under standard reaction conditions as previously described.[30,31] Briefly, a solution of 6 μmol Cys-MZHER_{2:342} was mixed with 8 μmol MAL-NOTA in 0.2N ammonium acetate solution. After reaction at room temperature for nearly 12hours, the NOTA-conjugated affibody were purified by preparative HPLC. The final product was lyophilized as a white powder. NOTA-MAL-MZHER_{2:342} was obtained in 50% yield. Matrixassisted laser desorption/ionization (MALDI) time-of-flight (TOF) mass spectrometry (MS) measured m/z 7791.0 for $[\text{MH}]^+$ (C₃₃₇H₅₃₄N₁₀₂O₁₀₇S₂, calculated molecular weight, 7790.1).

Radiolabeling

NOTA-MAL-MZHER_{2:342} was radiolabeled with ^{18}F following procedures [30,31] A solution of NOTA-MAL-MZHER_{2:342} Affibody molecule (300 μg , 38nmol) in sodium acetate buffer (20 μL , pH4, 0.2M) was added to a solution of AlCl₃ (6 μL , 2mM in sodium acetate buffer, pH4, 0.5M) and ^{18}F -fluoride (~3700MBq) in 100 μL target water. This mixture was heated for 15min at 100°C. After being diluted with water (10 mL), the reaction solution was transferred to a Varian BOND ELUT C18 column. The cartridge was washed with 10 mL water again, then the desired peptide was eluted with 0.3ml of 10mM HCl in ethanol. The product was reconstituted in saline and passed through a 0.22 μm Millipore filter into a sterile vial.

For quality control purposes, a portion of the product was diluted and injected onto an analytical C18 HPLC column to assay for radiochemical purity. The retention time for ^{18}F -Al-NOTA-MAL-MZHER_{2:342} was about 13min.

Cell Lines

Human ovarian cancer (SKOV-3) and breast cancer (JIMT-1, MCF-7) cell lines were purchased from Cell Bank of Shanghai Institutes for Biological Sciences. The cells were cultured in RPMI 1640 medium supplemented with 10% (v/v) heat-inactivated fetal bovine serum (GIBCO) (v/v) fetal bovine serum at 37 °C in an atmosphere containing 5% CO₂.

Competitive cell-binding assay

The in vitro binding characteristics of the ^{18}F -Al labeled affibody molecule were determined using displacement cell-binding assays.[21, 30] SKOV-3 tumor cells were cultured into six-well plates (2 × 10⁵ cells per well) until confluency. On the day of the assay, cells were washed with binding buffer (RPMI, 0.5% bovine serum albumin). Subsequently, the cells were incubated with ^{18}F -Al-NOTA-MAL-MZHER_{2:342} and increasing concentrations of non-labeled Cys-ZHER_{2:342} Affibody molecules. Removing medium at 2h incubation, cells were washed with binding buffer and collected for determining the radioactivity in a γ -counter (Perkin- Elmer). GraphPad Prism software [version 5.03 for Windows (Microsoft); GraphPad Software] was used to

calculate inhibitory concentration of 50% (IC50) values.

Animal Model

All animal experiments were approved by local authorities and were in compliance with the institutional guidelines. Approximately 5×10^6 tumor cells suspended in 0.2 mL PBS were subcutaneously implanted in the right front flank of 3–4 week-old female Balb/c nude mice (SLAC Laboratory Animal Co., Ltd., China). After tumor size reached 100–300 mm³, the animals were used for the following experiments.

MicroPET Imaging

Small-animal PET was performed with a microPET scanner (Siemens Inc.). Under isoflurane anesthesia, the mice were placed prone in the center of the field of view of the scanner and injected into 3.7 MBq ¹⁸FAl-NOTA-MAL-MZHER_{2:342} with or without excessive non-labeled Cys-MZHER_{2:342} via the lateral tail vein. Whole-body scanning was performed at different times after radiotracer injection and a 10-min static PET images were acquired. The quantification analysis of PET images was performed using the same method as previously reported. [30,31]

HER2 Western Analysis of Tumor Tissues

After microPET imaging, xenografted tumors were harvested and stored at -70°C. Allowing at least 48h for radioactive decay, the homogenized tissues were lysed using RIPA lysis buffer with 1mM PMSF. The supernatant were collected after centrifugation and used for HER2 Western Analysis. Estimated equal amount of the lysates were loaded in NuPAGE 10% Bis-Tris ReadyGel (Thermo Fisher Scientific Inc.) and transferred onto PVDF membrane (GE Healthcare, Piscataway, NJ, USA), then incubated at room temperature with 5% nonfat milk blocking buffer. The blots were incubated overnight at 4°C with rabbit anti-HER2 antibody (Beyotime), followed by incubation at room temperature for 1h with

horseradish peroxidase-conjugated anti-rabbit secondary antibody (Beyotime). The bands were detected using the BeyoECL plus Western blotting detection system (Beyotime). β -Actin was used as a loading control. Quantification analysis of western gel were performed according the literature.[32]

Biodistribution Studies

For biodistribution studies, mice were injected with 0.74 MBq of each radiotracer via the lateral tail vein. Among them, some mice were coinjected with an excess of unlabeled HER2 affibody (10mg/kg body weight). After euthanized by CO₂/O₂ asphyxiation, the mice were sacrificed at various time points from 30min to 4h postinjection. Tumor and major organs were dissected and weighed. Activity was measured in a γ -counter. The radioactivity uptakes in the organs were expressed as a percentage of the injected radioactive dose per gram of tissue (% ID/g).

Statistical Analysis

Statistical analyses were performed using GraphPad Prism. Data were analyzed using the unpaired, 2-tailed Student t test. Differences at the 95% confidence level ($p < 0.05$) were considered to be statistically significant.

Results

Chemistry

Cys-MZHER_{2:342} was readily conjugated with NOTA-MAL using a previously reported synthesis method. [30,31] Chemical purities of these compounds were >95 % determined by analytical HPLC analysis.

Radiochemistry

NOTA-MAL-MZHER_{2:342} was easily obtained by site-specific labeling with the Al¹⁸F complex in nearly 30min. The non-decay corrected yield was $9.3 \pm 1.5\%$ and radiochemical purity of more than 95% (Fig 2).

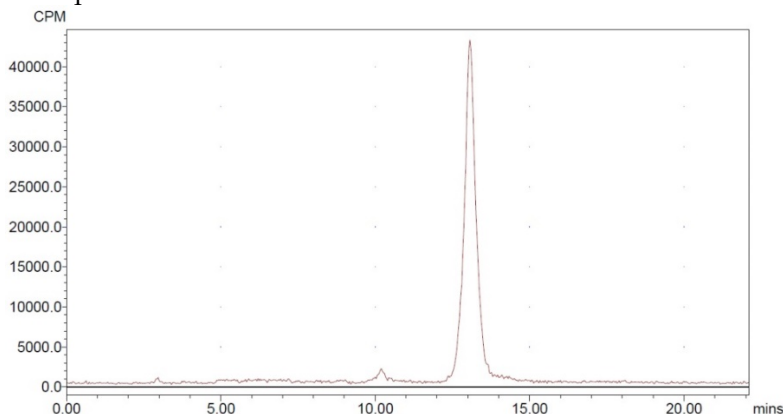


Figure 2. HPLC radiochromatogram of purified ¹⁸FAl-NOTA-MAL-MZHER_{2:342}

Binding specificity in vitro

The binding of ¹⁸FAl-NOTA-MAL-MZHER_{2:342} to the HER2 measured on SKOV-3 tumors was inhibited by various concentrations of non-labeled Cys-MZHER_{2:342}, and the IC₅₀ values were 116.71±1.28nM (Fig 3).

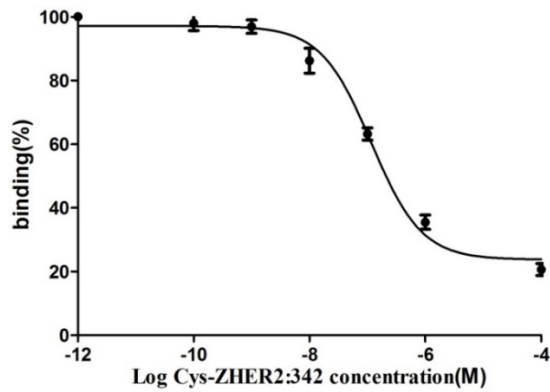


Figure 3. Competitive binding curves of IC₅₀ determination of ¹⁸FAl-NOTA-MAL-MZHER_{2:342} on SKOV-3 cells with Cys-ZHER_{2:342}

Small-Animal PET Imaging

Decay-corrected coronal microPET images of mice bearing SKOV-3 tumors were shown in Fig 4. Axial sections of mice with different levels of HER2 expression are displayed in Fig 5.

SKOV-3 and JIMT-1 xenografts were clearly visualized with good contrast after 1h injection. On the contrary, the tumor signals of MCF-7 tumor was difficult to visualize.

The ROI values ranged from 16.54±2.69% ID/g for SKOV-3 to 8.42±1.20% ID/g for JIMT-1 tumors at 1h postinjection respectively. Poor uptake was observed from MCF-7 tumors with 1.71±0.34% ID/g at the same time point. Excessive unlabeled Cys-ZHER_{2:342} decreased SKOV-3 tumor uptakes to 2.13±0.36% ID/g at 1h postinjection.

Quantitative analysis also revealed that the radioactivity uptake in the kidneys was significantly higher than in normal tissues, which ranged from 167.80±26.15% ID/g to 126.23±25.76% ID/g in mice bearing SKOV-3 and MCF-7 tumors at 1h postinjection respectively.

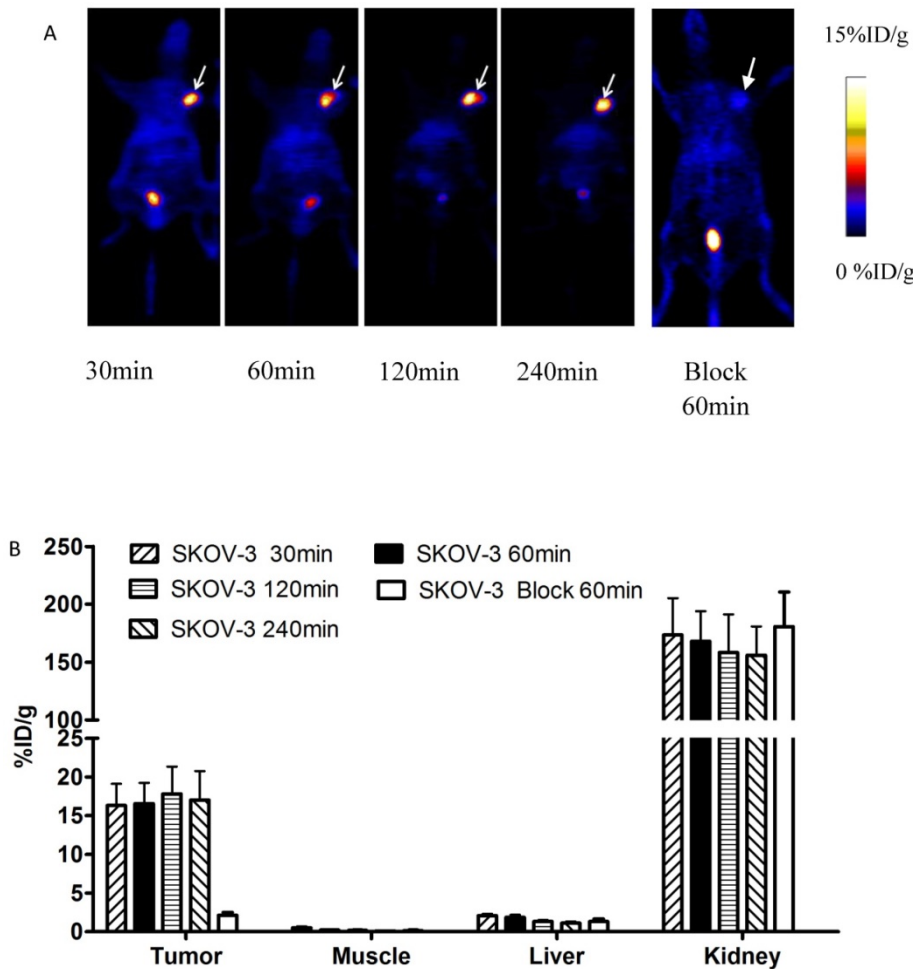


Figure 4. A) Decay-corrected whole-body PET images of mice bearing SKOV-3 xenografts after injection of ¹⁸FAl-NOTA-MAL-MZHER_{2:342} with or without block respectively. B) PET quantification analysis for uptakes of tumor, liver, kidney and muscles for ¹⁸FAl-NOTA-MAL-MZHER_{2:342}. ROIs are shown as mean %ID/g ± SD. Tumors are indicated by arrows.

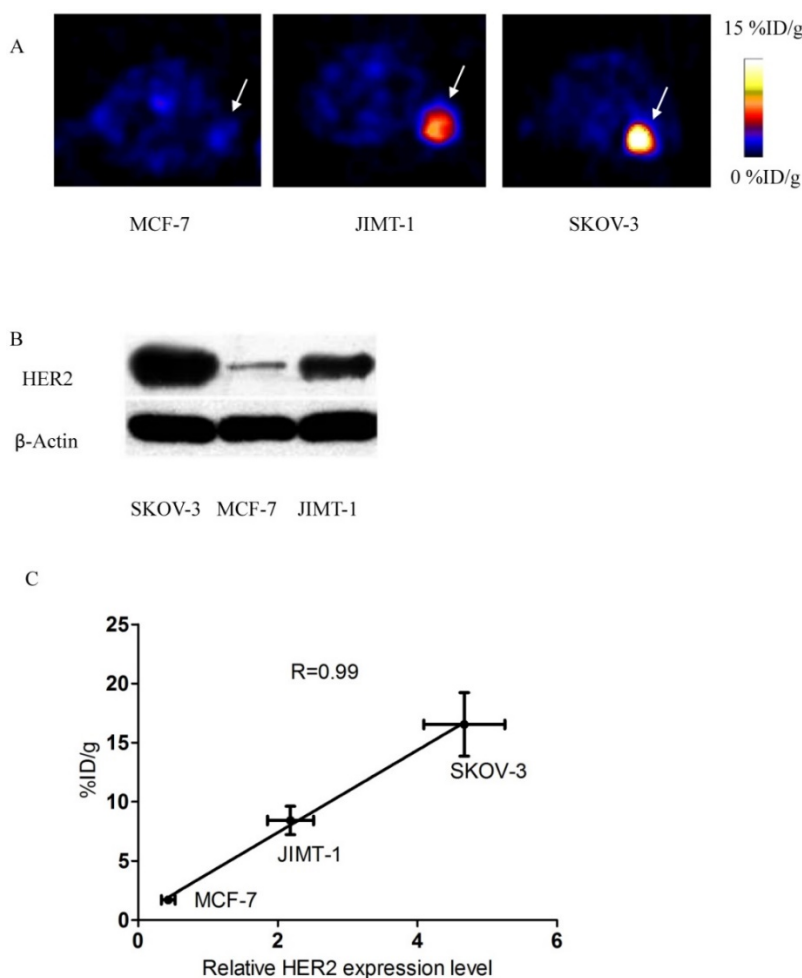


Figure 5. A) Axial sections 1 h after ^{18}F FAI-NOTA-MAL-MZHER_{2.342} injection in mice bearing tumors. B) Western blots of HER2 in SKOV-3, JIMT-1 and MCF7 xenografted tumors. C) Correlation of PET quantification of tumor uptake at 1 h after injection with relative HER2 expression levels.

Table 1. Biodistribution of ^{18}F FAI-NOTA-MAL-MZHER_{2.342}-Affibody in mice bearing SKOV-3, JIMT-1 and MCF-7 xenografts respectively.

Organ (%ID/g)	SKOV-3				SKOV-3 Block	MCF-7	JIMT-1
	30min	60min	120min	240min	60min	60min	60min
blood	1.26±0.10	0.65±0.08	0.39±0.07	0.19±0.01	0.47±0.06	0.55±0.06	0.69±0.12
brain	0.07±0.00	0.05±0.00	0.03±0.00	0.01±0.00	0.05±0.00	0.04±0.00	0.02±0.00
heart	0.55±0.06	0.31±0.06	0.19±0.01	0.09±0.01	0.27±0.03	0.36±0.03	0.15±0.02
liver	2.06±0.36	1.69±0.23	1.19±0.25	0.89±0.16	1.12±0.19	1.35±0.37	0.95±0.19
spleen	0.46±0.09	0.36±0.08	0.27±0.04	0.17±0.01	0.61±0.13	0.52±0.14	0.28±0.05
lung	1.23±0.24	0.67±0.06	0.43±0.09	0.23±0.02	0.81±0.08	0.50±0.04	0.93±0.09
kidney	167.16±26.28	176.09±12.67	183.65±34.52	133.65±21.89	139.80±19.56	149.25±15.52	153.88±24.71
stomach	0.69±0.08	0.46±0.04	0.47±0.11	0.27±0.03	0.59±0.07	0.39±0.02	0.36±0.08
intestine	0.93±0.23	0.56±0.12	0.34±0.04	0.14±0.02	0.79±0.12	0.74±0.14	0.23±0.09
muscle	0.47±0.17	0.31±0.08	0.12±0.03	0.08±0.00	0.18±0.03	0.26±0.06	0.22±0.05
pancreas	0.42±0.08	0.24±0.04	0.13±0.01	0.10±0.01	0.21±0.05	0.38±0.02	0.20±0.01
bone	1.40±0.17	1.34±0.08	0.64±0.12	0.44±0.05	0.99±0.11	0.64±0.19	1.03±0.15
tumor	18.32±3.22	18.60±3.89	19.09±4.77	17.82±2.46	1.89±0.26	1.96±0.41	9.50±2.13
Tumor/blood	14.83±1.73	29.80±4.65	52.84±11.71	94.80±9.35	4.15±0.58	3.68±0.64	14.75±2.65
Tumor/muscle	47.69±14.10	77.75±10.03	190.29±34.82	240.61±22.95	10.04±1.28	8.34±2.00	47.85±10.56

HER2 Western Analysis of Tumor Tissues

Western blots of HER2 in xenografted tumor samples were shown in Fig 5. HER2 was abundantly expressed in SKOV-3 and JIMT-1 tumors, but was significantly lower in MCF-7 tumors. Quantification

analysis of western gel further revealed that relative HER2 expression level was 4.67 ± 0.58 , 2.18 ± 0.33 and 0.43 ± 0.10 in SKOV3, JIMT-1 and MCF-7 tumors respectively.

Besides, a significant linear correlation between % ID/g values and relative HER2 expression level

obtained from PET quantification and Western analysis respectively was found ($R^2=0.99$, $p<0.05$) in all tumor-bearing mice.

Biodistribution Studies

The *in vivo* tumor targeting and imaging profile of ^{18}F FAI-NOTA-MAL-MZHER_{2:342} was further investigated by *ex vivo* biodistribution studies (Table 1). Biodistribution data were consistent with the imaging data and showed that the uptake of the Al¹⁸F labeled MZHER_{2:342} was $18.32\pm 3.22\%$ ID/g at 30min and kept stable to $17.82\pm 2.46\%$ ID/g in SKOV-3 tumors at 4h postinjection. Accumulation of radioactivities in the JIMT-1 and MCF-7 models was $9.50\pm 2.13\%$ ID/g and $1.96\pm 0.41\%$ ID/g at 1 h after administration. The coinjection of Cys-ZHER_{2:342} dramatically reduced the SKOV-3 tumor uptake of the tracer to $1.89 \pm 0.26\%$ ID/g at 1 h after injection.

Lower levels of radioactivity were observed in the blood and most other organs. Tumor-to-muscle and tumor-to-blood ratios in mice bearing SKOV-3, JIMT-1 and MCF-7 xenografts were 29.80 ± 4.65 , 3.68 ± 0.64 , 14.75 ± 2.65 and 190.29 ± 34.82 , 8.34 ± 2.00 , 47.85 ± 10.56 at 1h p.i. The uptakes in the liver was $1.69\pm 0.23\%$ ID/g at 1h after injection in SKOV-3, and was similar to those in JIMT-1 and MCF-7 models ($1.35\pm 0.37\%$ ID/g and $0.95\pm 0.19\%$ ID/g respectively). Among the normal tissues, high activity accumulation was also found in the kidney for all models, which was agreement to the finding from the imaging study. These data confirmed that ^{18}F FAI labeled MZHER_{2:342} were mainly cleared via the urinary system.

Discussion

Molecular imaging with ^{18}F labeled HER2 affibody analogs has shown great potential for tumor characterization and treatment monitoring. Nevertheless, unfavorable hepatic excretion of the tracers may affect the tumor-to-normal tissue ratios and decrease the contrast. Modification the affibody molecule with a hydrophilic linker might effectively alter the pharmacokinetics. [24, 25]

In the present study, only one pot reaction was performed in synthesizing the ^{18}F FAI labeled derivative of ZHER_{2:342}, and the total preparation time was about 30min with a non-decay-corrected yield at the end of synthesis of 10%. Regarding the aspect of radiosynthesis, the tracer was superior to ^{18}F -FBEM-ZHER_{2:342} (2 hours preparation time and 6.5% radiochemical yield) [21]. Satisfactory radiochemical purities were achieved by analytical radio-HPLC, which revealed that a Sep-Pak C18 cartridge was enough for purification of ^{18}F FAI labeled HER_{2:342} without further HPLC separation.

SKOV-3 tumor is always employed for

evaluating the biologic properties of radiolabeled HER2 affibody due to abundant HER2 expression.[33,34,35] Thus the HER2 targeting characteristic of ^{18}F FAI-NOTA-MAL-MZHER_{2:342} was initially determined using SKOV-3 models.

In vitro competitive cell-binding experiments showed that the IC₅₀ value of ^{18}F FAI-NOTA-MAL-MZHER_{2:342} was slightly lower than that of ^{18}F -FBEM-ZHER_{2:342} (116.71 nM vs ~170nM) under similar assay procedure using Cys-ZHER_{2:342} as competitor with increasing concentrations. [21] It demonstrated that the modification was to have a minimal effect on receptor binding. Also, it indicated that the *in vivo* tumor-specific uptake characteristics of ^{18}F FAI labeled affibody might be more somewhat favorable.

Considering the interesting findings *in vitro*, the biological characters of the probe were further investigated in living mice bearing tumors using MicroPET imaging. SKOV-3 xenografts are clearly delineated from the surround normal tissues from 30 minutes to 4 hours after injection. Quantification of small-animal PET images showed that nearly 90% of the activity remains in the tumor at 4 h after injection. PET images also showed that even at 4 h after injection, the SKOV-3 tumor uptake of ^{18}F FAI-NOTA-MAL-MZHER_{2:342} can also achieve approximately 15% ID/g, which was significantly higher than those of reported ^{18}F labeled ZHER_{2:342} affibody.(~6% ID/g at 4h p.i.).[21] Meanwhile, coinjection with excess of unlabeled ZHER_{2:342} affibody dramatically decreased the SKOV-3 tumor uptake and the imaging quality. These results confirmed the excellent receptor targeting specificity of the ^{18}F FAI labeled ZHER_{2:342} affibody as assessed by *in vitro* methods.

To further determine whether the radiolabeled ZHER_{2:342} affibody can play a complementary role in assessing target expression, the biological properties of the tracer were also tested in tumors with different HER2 expressions. Similar with the literature, *in vivo* PET values for each particular tumor model also corresponds well with the HER2 expression levels. [35]A significant linear dependence was found between the retained values of the probe and HER2 status in the tumors. The uptake values in SKOV-3 tumors were nearly 2 and 10 folds higher than those of JIMT-1 and MCF-7 tumors respectively, which was consistent with the outcomes of HER2 Western analysis. It means that ^{18}F FAI labeled MZHER_{2:342} affibody molecules may own favorable sensitivity to detect differences in HER2 expression levels.

Biodistribution results were agreement with the PET data analysis, ^{18}F FAI-NOTA-MAL-MZHER_{2:342} rapidly localized in HER2-positive tumors and was

eliminated quickly from the blood and normal tissues. The tumor-to-blood and tumor-to-muscle ratios were significantly higher than those of reported ^{18}F labeled HER2 affibody at 60min postinjection (29.80 ± 4.65 and 77.75 ± 10.03 vs 7.5 ± 4.5 and 21 ± 4.7 respectively, $p < 0.01$). At the same time points, ^{18}F FAI-NOTA-MAL-MZHER_{2:342}, compared with ^{18}F -FBEM-ZHER_{2:342}, exhibits significantly reduced accumulation in the livers (almost 2% ID/g vs. 5% ID/g at 1 h respectively) [21]. It confirmed that modification of the affibody molecules with the hydrophilic linker could reduce hepatobiliary excretion, optimize contrast and improve image quality.

Renal system was the prominent excretion profiles. Enhanced radioactivity accumulation is comparable to those previously reported for ^{64}Cu or ^{68}Ga labeled affibody molecules. [36,37] Considering the physical half-life, positron energy and range, radiation burden of the ^{18}F FAI labeled MZHER_{2:342} affibody may be lower than those of the metal labeled counterparts. Although the kidney is the major dose-limiting organ for the probe, renal protection could be performed by the use of positively charged amino acids, gelofusin, or albumin fragments. Possible effect of the following compounds is under active investigation.

^{18}F FAI-NOTA-MAL-MZHER_{2:342} also produced lower level of radioactivity ($< 1\%$ ID/g) in the bone than those of ^{18}F -FBEM-ZHER_{2:342} (2% ID/g) at 1h postinjection as a result of in vivo stability of the tracer. [21] Thus, the tracer may decrease the background signal for detection of bone metastasis and radiation dose to the bone marrow.

Conclusion

A novel HER2 affibody, ^{18}F FAI-NOTA-MAL-MZHER_{2:342} has been successfully obtained by a simple route. The tracer shows favorable profiles and excellent tumor imaging quality. It demonstrated that differences in HER2 expression levels can be detected in vivo by PET imaging with the tracer. Therefore, ^{18}F FAI labeled ZHER_{2:342} may be useful in providing specific information on the receptor expression of cancers.

Acknowledgment

This work was partially supported by National Natural Science Foundation (81472749, 81171399, 81101077, 51473071, 81401450, 21401084), CSC Foundation (2011832173), National Significant New Drugs Creation Program (2012ZX09505-001-001), Jiangsu Province Science and Technology Foundation (BE2012622, BE2016632, BK2011166, BE2014609 and BL2012031), Health Ministry of Jiangsu Province

Fund (RC2011095, H201529 and H201028), Public service platform for Science and technology infrastructure construction project of Jiangsu Province (BM2012066), University of Wisconsin-Madison Department of Medical Physics and Department of Radiology (Radiology R&D Award 1105-002).

Competing Interests

The authors have declared that no competing interest exists.

References

- Zidan J, Dashkovsky I, Stayerman C, et al. Comparison of HER-2 overexpression in primary breast cancer and metastatic sites and its effect on biological targeting therapy of metastatic disease. *Br J Cancer*. 2005;93:552-6.
- Rimawi MF, Schiff R, Osborne CK. Targeting HER2 for the treatment of breast cancer. *Annu Rev Med*. 2015;66:111-28.
- Friedlander E, Barok M, Szollosi J, et al. ErbB-directed immunotherapy: antibodies in current practice and promising new agents. *Immunol Lett*. 2008; 116:126-40.
- Teplinsky E, Muggia F. Targeting HER2 in ovarian and uterine cancers: challenges and future directions. *Gynecol Oncol*. 2014; 135:364-70.
- Tuma RS. Inconsistency of HER2 test raises questions. *J Natl Cancer Inst*. 2007; 99:1064-5.
- Gaykema SB, Schröder CP, Vitfell-Rasmussen J, et al. ^{89}Zr -trastuzumab and ^{89}Zr -bevacizumab PET to evaluate the effect of the HSP90 inhibitor NVP-AUY922 in metastatic breast cancer patients. *Clin Cancer Res*. 2014;20:3945-54.
- Marquez BV1, Ikotun OF, Zheleznyak A, et al. Evaluation of (^{89}Zr)-pertuzumab in Breast cancer xenografts. *Mol Pharm*. 2014;11:3988-95.
- Jain M, Kamal N, Batra SK. Engineering antibodies for clinical applications. *Trends Biotechnol*. 2007;25:307-16.
- Orlova A, Wällberg H, Stone-Elander S, et al. On the selection of a tracer for PET imaging of HER2-expressing tumors: direct comparison of a ^{124}I -labeled affibody molecule and trastuzumab in a murine xenograft model. *J Nucl Med*. 2009;50:417-25.
- Su X, Cheng K, Jeon J, et al. Comparison of two site-specifically (^{18}F)-labeled affibodies for PET imaging of EGFR positive tumors. *Mol Pharm*. 2014;11:3947-56.
- Feldwisch J, Tolmachev V. Engineering of affibody molecules for therapy and diagnostics. *Methods Mol Biol*. 2012; 899:103-26.
- Löfblom J, Feldwisch J, Tolmachev V, et al. Affibody molecules: engineered proteins for therapeutic, diagnostic and biotechnological applications. *FEBS Lett*. 2010;584:2670-80.
- Ahlgren S1, Orlova A, Wällberg H, et al. Targeting of HER2-expressing tumors using 111In-ABY-025, a second-generation affibody molecule with a fundamentally reengineered scaffold. *J Nucl Med*. 2010;51:1131-8.
- Eigenbrot C, Ultsch M, Dubnovitsky A, et al. Structural basis for high-affinity HER2 receptor binding by an engineered protein. *Proc Natl Acad Sci U S A*. 2010;107:15039-44.
- Altai M, Honarvar H, Wällberg H, et al. Selection of an optimal cysteine-containing peptide-based chelator for labeling of affibody molecules with (^{188}Re). *Eur J Med Chem*. 2014;87:519-28.
- Lindberg H, Hofström C, Altai M, et al. Evaluation of a HER2-targeting affibody molecule combining an N-terminal HEHEHE-tag with a GGGC chelator for $^{99\text{m}}\text{Tc}$ -labelling at the C terminus. *Tumour Biol*. 2012;33:641-51.
- Sörensen J, Sandberg D, Sandström M, et al. First-in-human molecular imaging of HER2 expression in breast cancer metastases using the ^{111}In -ABY-025 affibody molecule. *J Nucl Med*. 2014;55:730-5.
- Zhang JM, Zhao XM, Wang SJ, et al. Evaluation of $^{99\text{m}}\text{Tc}$ -peptide-ZHER2:342 Affibody® molecule for in vivo molecular imaging. *Br J Radiol*. 2014;87:20130484.
- Kramer-Marek G, Shenoy N, Seidel J, et al. ^{68}Ga -DOTA-affibody molecule for in vivo assessment of HER2/neu expression with PET. *Eur J Nucl Med Mol Imaging*. 2011;38:1967-76.
- Miao Z, Ren G, Liu H, et al. Small-animal PET imaging of human epidermal growth factor receptor positive tumor with a ^{64}Cu labeled affibody protein. *Bioconjug Chem*. 2010;21:947-54.
- Kramer-Marek G, Kiesewetter DO, Martiniova L, et al. [^{18}F]FBEM-Z(HER2:342)-Affibody molecule-a new molecular tracer for in vivo monitoring of HER2 expression by positron emission tomography. *Eur J Nucl Med Mol Imaging*. 2008; 35:1008-18.
- Kramer-Marek G, Bernardo M, Kiesewetter DO, et al. PET of HER2-positive pulmonary metastases with ^{18}F -ZHER2:342 affibody in a murine model of breast cancer: comparison with ^{18}F -FDG. *J Nucl Med*. 2012;53:939-46.
- Kramer-Marek G, Gijzen M, Kiesewetter DO, et al. Potential of PET to predict the response to trastuzumab treatment in an ErbB2-positive human xenograft tumor model. *J Nucl Med*. 2012;53:629-37.

24. Yang M, Gao H, Zhou Y, et al. 18F-Labeled GRPR Agonists and Antagonists: A Comparative Study in Prostate Cancer Imaging. *Theranostics*. 2011;1:220-9.
25. Pan D, Xu YP, Yang RH, et al. A new (68)Ga-labeled BBN peptide with a hydrophilic linker for GRPR-targeted tumor imaging. *Amino Acids*. 2014;46:1481-9.
26. Pan D, Yan Y, Yang R, et al. PET imaging of prostate tumors with 18F-Al-NOTA-MATBBN. *Contrast Media Mol Imaging*. 2014; 9:342-8.
27. McBride WJ, Sharkey RM, Goldenberg DM. Radiofluorination using aluminum-fluoride (Al18F). *EJNMMI Res*. 2013;3(1):36.
28. Wan W, Guo N, Pan D, et al. First experience of 18F-alfatide in lung cancer patients using a new lyophilized kit for rapid radiofluorination. *J Nucl Med*. 2013;54:691-8.
29. Glaser M, Iveson P, Hoppmann S, et al. Three methods for 18F labeling of the HER2-binding affibody molecule Z(HER2:2891) including preclinical assessment. *J Nucl Med*. 2013;54:1981-8.
30. Xu Q, Zhu C, Xu Y, et al. Preliminary evaluation of [18F]AlF-NOTA-MAL-Cys39-exendin-4 in insulinoma with PET. *J Drug Target*. 2015;23:813-20.
31. Xu Y, Pan D, Zhu C, et al. Pilot study of a novel (18)F-labeled FSHR probe for tumor imaging. *Mol Imaging Biol*. 2014;16:578-85.
32. Miao Z, Ren G, Liu H, et al. PET of EGFR expression with an 18F-labeled affibody molecule. *J Nucl Med*. 2012;53:1110-8.
33. Westerlund K, Honarvar H, Norrström E, et al. Increasing the Net Negative Charge by Replacement of DOTA Chelator with DOTAGA Improves the Biodistribution of Radiolabeled Second-Generation Synthetic Affibody Molecules. *Mol Pharm*. 2016;13 :1668-78.
34. Honarvar H, Westerlund K, Altai M, et al. Feasibility of Affibody Molecule-Based PNA-Mediated Radionuclide Pretargeting of Malignant Tumors. *Theranostics*. 2016;6:93-103.
35. Kramer-Marek G, Shenoy N, Seidel J, et al. 68Ga-DOTA-affibody molecule for in vivo assessment of HER2/neu expression with PET. *Eur J Nucl Med Mol Imaging*. 2011;38:1967-76.
36. Altai M, Strand J, Rosik D, et al. Influence of nuclides and chelators on imaging using affibody molecules: comparative evaluation of recombinant affibody molecules site-specifically labeled with ⁶⁸Ga and ¹¹¹In via maleimido derivatives of DOTA and NODAGA. *Bioconjug Chem*. 2013;24:1102-9.
37. Cheng Z, De Jesus OP, Kramer DJ, et al. 64Cu-labeled affibody molecules for imaging of HER2 expressing tumors. *Mol Imaging Biol*. 2010;12:316-24.